



HAL
open science

Combination of linear solvation energy and linear free-energy relationships to aid the prediction of reaction kinetics: application to the solvolysis of 5-HMF by alcohol to levulinate

Erny Encarnacion Munoz, Daniele Di Menno Di Bucchianico, Christine Devouge-Boyer, Julien Legros, Christoph Held, Jean-Christophe Buvat, Valeria Casson Moreno, Sébastien Leveneur

► To cite this version:

Erny Encarnacion Munoz, Daniele Di Menno Di Bucchianico, Christine Devouge-Boyer, Julien Legros, Christoph Held, et al.. Combination of linear solvation energy and linear free-energy relationships to aid the prediction of reaction kinetics: application to the solvolysis of 5-HMF by alcohol to levulinate. *Chemical Engineering Research and Design*, 2024, 205, pp.312-323. 10.1016/j.cherd.2024.03.040 . hal-04527410

HAL Id: hal-04527410

<https://hal.science/hal-04527410>

Submitted on 18 Apr 2024

HAL is a multi-disciplinary open access archive for the deposit and dissemination of scientific research documents, whether they are published or not. The documents may come from teaching and research institutions in France or abroad, or from public or private research centers.

L'archive ouverte pluridisciplinaire **HAL**, est destinée au dépôt et à la diffusion de documents scientifiques de niveau recherche, publiés ou non, émanant des établissements d'enseignement et de recherche français ou étrangers, des laboratoires publics ou privés.



Combination of linear solvation energy and linear free-energy relationships to aid the prediction of reaction kinetics: Application to the solvolysis of 5-HMF by alcohol to levulinate

Erny Encarnacion Munoz^a, Daniele Di Menno Di Bucchianico^{a,b}, Christine Devouge-Boyer^d, Julien Legros^d, Christoph Held^e, Jean-Christophe Buvat^a, Valeria Casson Moreno^c, Sébastien Leveneur^{a,*}

^a INSA Rouen Normandie, Univ Rouen Normandie, Normandie Univ, LSPC UR 4704, Rouen F-76000, France

^b Dipartimento di Ingegneria Chimica, Civile, Ambientale e dei Materiali, Alma Mater Studiorum—Università di Bologna, via Terracini 28, Bologna 40131, Italy

^c Department of Civil and Industrial Engineering, University of Pisa, Largo Lucio Lazzarino n. 1, Pisa 56126, Italy

^d Univ Rouen Normandie, INSA Rouen Normandie, CNRS, Normandie Univ, COBRA, Rouen F-76000, France

^e Laboratory of Thermodynamics, Department of Biochemical and Chemical Engineering, TU Dortmund University, Emil-Figge Str.70, Dortmund 44227, Germany

ARTICLE INFO

Keywords:
Taft equation
KAT
Kinetic modeling
Levulinates
Reaction medium effect

ABSTRACT

In the context of cellulose valorization, we studied the kinetics of levulinates synthesis via the solvolysis of 5-HMF by alcohol over Amberlite IR-120. The alcohol plays a double role; it is a reactant and acts as the solvent. In the literature, kinetic models were developed for each type of alcohol, but there were no models combining the dual effect of alcohol alkyl group substituent (ROH) as a reactant and solvent. Such global kinetic models can save time and optimize a process by considering the solvent effect. This effect was taken into account via the Kamlet–Abboud–Taft and Taft equations, using Bayesian inference. We studied the kinetics of levulinate production from 5-HMF in a reaction mixture made of alcohol and GVL within a temperature range from 80 to 115 °C. The following alcohols were used: methanol, ethanol, propanol, butanol, pentanol, and hexanol. It was found that the rate of alkyl levulinate production increases faster in alcohol reaction medium compared to water reaction medium, and increases when increasing the alkyl group substitution ($r_{ML}^{Methanol} > r_{EL}^{Ethanol} > r_{PL}^{Propanol} > r_{BL}^{Butanol} > r_{PeL}^{Pentanol} > r_{HeL}^{Hexanol} > r_{LA}^{Water}$). Among the global kinetic models developed in this study, the one that neglects the side reaction of humins was found to be the most reliable.

1. Introduction

Valorization of biomass contributes to decreasing our dependency on fossil raw materials. There are mainly three different technology approaches, which are pyrolysis (Gogoi et al., 2023; Ayub et al., 2023), gasification (Ayub et al., 2023; Verma et al., 2023; Yan et al., 2021) or chemical and enzymatic valorization (Ning et al., 2021), also known as hydrolysis. For the chemical and enzymatic routes, the sugar fraction (cellulose or hemicellulose) or simple sugars (glucose, fructose, etc.) are the most valorized, and can lead to several chemicals and platform molecules like 5-(hydroxymethyl) furfural (5-HMF), sorbitol, alcohol (ethanol, butanol, etc.) or levulinic acid or alkyl levulinates (Takkellapati et al., 2018; Wu et al., 2023). The production of any of these platform molecules depends on the operating conditions, solvent and

catalyst.

In the valorization of cellulose or hemicellulose, solvent plays several fundamental roles in depolymerization stages, sugar solubilization, and as reactant. It is the case for the production of 5-(hydroxymethyl) furfural (5-HMF)/levulinic acid (LA) or 5-(alkoxymethyl) furfural (RMF) or alkyl levulinates (RL). The alcohol (ROH) or water influences the solubility of simple sugars like fructose or glucose but also orients the final product, i.e., methyl levulinate if methanol is used, ethyl levulinate if ethanol is used, and so on (Di Menno Di Bucchianico et al., 2022a).

Alkyl levulinates are promising platform molecules identified as potential biofuels and fuel additives (Chen et al., 2019; Karnjanakom et al., 2021; Chithra and Darbha, 2020; Yu et al., 2019; Flannelly et al., 2015; Sajid et al., 2021; Ahmad et al., 2022; Delidovich et al., 2014). They could also be used in the food industry because the combination of LA and sodium dodecyl sulfate is a promising antimicrobial agent (Zhou

* Corresponding author.

E-mail address: sebastien.leveneur@insa-rouen.fr (S. Leveneur).

<https://doi.org/10.1016/j.cherd.2024.03.040>

Received 30 January 2024; Received in revised form 14 March 2024; Accepted 26 March 2024

Available online 30 March 2024

0263-8762/© 2024 The Author

S

. Published by Elsevier Ltd on behalf of Institution of Chemical Engineers. This is an open access article under the CC BY-NC-ND license (<http://creativecommons.org/licenses/by-nc-nd/4.0/>).

From the linear solvation energy relationships (LSERs), they developed a quantitative measure of solvent polarity effect by considering three parameters: solvent capacity to donate hydrogen bonds, solvent capacity to accept hydrogen bonds, and solvent capacity to stabilize or destabilize charges and dipoles.

As mentioned, in the case of RL and 5-RMF production from simple sugar solvolysis by alcohol, alcohol (ROH) plays a double role: solvent and reactant. The motivation of our study was to develop kinetic models considering the dual role of alcohol reaction medium. Our study started with the solvolysis of 5-HMF (Fig. 1) to avoid interference from the complex fructose or glucose dissolution mechanism. The KAT relationships were used to describe the solvent effect, and the Taft equation was used to explain the reactant effect between the substituent R- and the kinetics (Kamlet et al., 2007; Taft, 1952a, 1952b, 1953a, 1953b). Taft showed three main contributions of the substituent R- on the reaction center: the polar, steric and resonance effects. The use of the Taft equation in kinetic modeling has successfully been applied in several reactions, such as esterification (Lilja et al., 2002; Vojtko and Tomčík, 2014) or hydrogenation (Wang et al., 2019).

To the best of our knowledge, it is the first time that a kinetic model includes the solvent effect via the KAT equation and the substituent R-effect via the Taft equation. Such an approach could save time for the kinetic modeling stage by combining substituent and solvent effects on kinetics. A previous study of our group shows that Amberlite IR-120 is an efficient catalyst for this reaction system, and using GVL as a co-solvent is beneficial for this reaction system (Di Menno Di Bucchianico et al., 2023, 2022a, 2022b). In this study, kinetic models of the 5-HMF solvolysis over Amberlite IR-120 in a reaction medium constituted of 70 wt% of alcohol and 30 wt% of GVL were developed. Di Menno Di Bucchianico et al (Di Menno Di Bucchianico et al., 2022b). showed that this alcohol/GVL ratio gave the best results from a kinetic standpoint. Water and different alcohols such as methanol, ethanol, propanol, n-butanol, pentanol and hexanol were used.

2. Experimental section

2.1. Chemicals

All the chemicals used as reagents and solvents are listed in Table 1, along with their purity and supplier. The Amberlite IR-120 H+ form (ion-exchange resin, 94 % of particle have a native particle size range (μm): 300–1180 μm) commercial catalyst was purchased from Thermo Scientific. Nitrogen gas (N_2 , purity > 99.999 vol %) came from Linde.

Table 1

List of chemicals used in this work as reagents and solvents.

Chemicals	Acronym	Purity, wt%	Supplier
5-(hydroxymethyl) furfural	5-HMF	96	Apollo Scientific
5-(ethoxymethyl) furfural	EMF	97	Sigma-Aldrich
levulinic acid	LA	≥ 97	Sigma-Aldrich
γ -valerolactone	GVL	≥ 99	Sigma-Aldrich
methanol	MeOH	≥ 99.8	Merck
ethanol	EtOH	≥ 99.5	Merck
1-propanol	PrOH	≥ 99.7	Merck
1-butanol	BuOH	≥ 99.5	Merck
1-pentanol	PeOH	≥ 99	Merck
1-hexanol	HeOH	≥ 98	Merck
methyl levulinate	ML	≥ 98.0	Sigma-Aldrich
ethyl levulinate	EL	≥ 99	Sigma-Aldrich
propyl levulinate	PL	≥ 95	Sigma-Aldrich
butyl levulinate	BL	≥ 98	Sigma-Aldrich
methyl formate	MF	≥ 97	Sigma-Aldrich
ethyl formate	EF	≥ 97	Sigma-Aldrich
propyl formate	PF	≥ 97	Sigma-Aldrich
butyl formate	BF	≥ 97	Sigma-Aldrich
acetone	-	≥ 99.9	Sigma-Aldrich

All chemicals were employed without further purification.

2.2. Analytical methods

Reaction samples were diluted in acetone and analyzed by a gas chromatograph Scion 456 GC, equipped with a VF-1701 ms Agilent column (60.0 m length \times 250 μm inner diameter \times 0.25 μm film thickness) and a flame ionization detector (FID). The injector was set with a temperature of 250 $^{\circ}\text{C}$, injection volume of 1 μL , and a split ratio of 1:20. Helium (>99.999 vol %) is used as the carrier gas at a constant flow rate of 1.0 ML/min to transfer the sample from the injector through the column and into the FID detector, whose temperature was set to 250 $^{\circ}\text{C}$. The oven temperature was programmed from 40 to 240 $^{\circ}\text{C}$ with 20 $^{\circ}\text{C}/\text{min}$ of ramp rate. Reference samples with standard solutions of pure 5-HMF, LA, EMF and the corresponding alkyl levulinate were used as standards to prepare daily calibration curves. EMF and BL were used as the standard for concentrations of 5-(methoxymethyl) furfural (MMF), 5-(propoxymethyl) furfural (PMF), 5-(butoxymethyl) furfural (BMF), 5-(pentoxymethyl) furfural (PeMH), 5-(hexoxymethyl) furfural (HeMF), hexyl levulinate (HL), pentyl levulinate (PeL) and propyl levulinate (PL) due to their commercial unavailability. Each sample was measured three times on the GC, the standard deviation of the measured concentrations

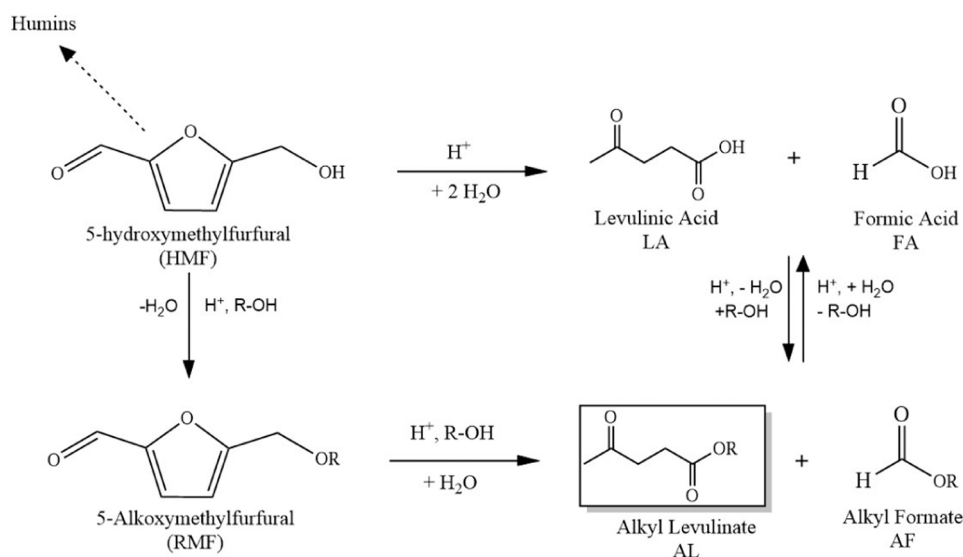


Fig. 1. Pathway for 5-HMF conversion to levulinic acid and alkyl levulinate.

was around 0.03 mol/L.

2.3. Kinetic experiments

Kinetic experiments were performed under isobaric and controlled-temperature conditions in a 300 ML stainless steel batch reactor. The reactor was equipped with an electrical heating jacket, a cooling coil, and a thermocouple capable of measuring the reaction temperature and communicating with the temperature controller. The presence of a gas entrainment impeller (diameter 2.5 cm) with a hollow shaft provided a uniform mixing of the mixture.

As shown in Table 2 for each experiment, the reactor was loaded with 5-HMF initial mass varying between 4 and 5 g, a catalyst loading varying between 2.5 and 4 g and a fixed volume with a ratio of 70/30 %wt alcohol/GVL were used (Di Menno Di Bucchianico et al., 2022a). The rotation speed was set to 800 rpm, since previous studies by Di Menno Di Bucchianico et al. (2022b). on fructose butanolysis using Amberlite IR120 in the same apparatus have demonstrated the negligibility of external and internal mass transfer limitations by using the native catalyst particle size distribution ($\geq 94\%$, particle diameters between 300 and 1180 μm) at this agitation speed (Di Menno Di Bucchianico et al., 2022b). For each kinetic experiment (Table 2) fresh catalyst was used; before its use the catalyst was washed with distilled water and then with the pure corresponding alcohol, then dried in an oven for 5 h (Di Menno Di Bucchianico et al., 2022b).

After loading the reaction mixture, catalyst and assembling the reactor, the system was pressurized with nitrogen at 20 bars to avoid any vaporization of the reaction mixture. Then, the temperature heater and rotation stirrer were switched on, and it was defined at time zero. It is essential to stress that when the rotation stirrer was switched on, the time to reach the desired temperature could vary between 15 and 20 minutes. This temperature variation was considered in the modeling, and samples were collected at ambient temperature, 60 °C, 90 °C, then when the desired temperature was reached a sample was taken, and then every hour up to 7 h.

In kinetic experiments, the temperature was set between 80 and 110 °C, without exceeding 120 °C. In fact, active sulfonic sites from Amberlite IR-120 can leach for temperatures higher than 120 °C (Di Menno Di Bucchianico et al., 2023).

2.4. Structure reactivity relationships

For the Taft equation, the substituent Me- is the reference one. Thus, we needed to express all relationships towards this substituent and in the methanol reaction medium.

Table 2

Experimental matrix with initial conditions.*

Run	Temp (°C)	mHMF ₀ (g)	mROH ₀ (g)	mGVL ₀ (g)	mdried cat (g)	[GVL] ₀ (mol/L)	[ROH] ₀ (mol/L)	[HMF] ₀ (mol/L)	Alcohol
1	100	5	83.71	35.88	4	2.27	16.58	0.28	MeOH
2	110	5	83.71	35.88	4	2.27	16.58	0.27	MeOH
3	100	5	83.6	35.8	4	2.27	11.51	0.30	EtOH
4	110	5	83.6	35.8	4	2.27	11.51	0.27	EtOH
5	100	5	84.67	36.29	4	2.31	8.99	0.26	PrOH
6	110	5	84.67	36.29	4	2.31	8.99	0.28	PrOH
7	100	5	85.22	36.53	4	2.33	7.34	0.26	n-BuOH
8	110	5	85.22	36.53	4	2.33	7.34	0.27	n-BuOH
9	100	5	85.22	36.53	4	2.33	6.17	0.26	n-PeOH
10	110	5	85.22	36.53	4	2.33	6.17	0.26	n-PeOH
11	90	5	83.71	35.88	4	2.27	16.58	0.34	MeOH
12	100	5	83.6	35.8	4	2.27	11.51	0.28	EtOH
13	90	5	83.6	35.8	4	2.27	11.51	0.28	EtOH
14	90	5	85.22	36.53	4	2.33	6.17	0.25	n-PeOH
15	85	4	83.71	35.88	3.5	2.29	16.72	0.22	MeOH
16	80	4	85.22	36.53	2.5	2.33	7.34	0.20	n-BuOH
17	100	5	85.54	36.66	4	2.36	5.39	0.26	n-HeOH
18	110	5	85.54	36.66	4	2.36	5.39	0.25	n-HeOH

* [RMF]₀ and [RL]₀ initial concentrations are zero in every Run.

2.4.1. Taft equation

Based on linear free-energy relationships (LFER), this equation allows predicting kinetic or thermodynamic constants of a chemical reaction based on reactant structure. The LFER is used for a congeneric series of compounds that share the same reaction center or functional group for a specific reaction; such groups can be –SH, –COOH and –CO, etc (Leveneuer, 2017). In our system, alcohols share the same functional group –OH, meaning we can use the LFER to relate their reactivity and structure for different reactions.

$$\log \frac{k_{X-R}^{\text{MeOH}}(T)}{k_{X-\text{Me}}^{\text{MeOH}}(T)} = \rho_X^{\text{MeOH}} \cdot \sigma^*(-R) + \delta_X^{\text{MeOH}} \cdot E_s(-R) + \Psi_X^{\text{MeOH}} \quad (1)$$

where, $k_{X-R}^{\text{MeOH}}(T)$ is the rate constant at a temperature T of a reaction X involving the substituent –R in methanol reaction medium. The terms $k_{X-\text{Me}}^{\text{MeOH}}(T)$ is the rate constant of reaction X at the same temperature T of the same reaction but involving the reference substituent in methanol reaction medium, which is the methyl group (CH₃-) for Taft equation. The term $\sigma^*(-R)$ represents the net polar effect of the substituent –R on the functional group or reaction center. It measures the inductive electron-withdrawing or –donating towards the functional group or reaction center. The term ρ_X^{MeOH} measures the importance of the polar effect on a given reaction series X in methanol reaction medium. The term $E_s(-R)$ represents the total steric effect due to the substituent –R on the functional group or reaction center. The term δ_X^{MeOH} evaluates the importance of steric effect for a given reaction series. The term Ψ_X^{MeOH} describes the resonance effect between the substituent and the reaction center. In this study, there is no resonance between the selected substituents and reaction center/functional group. The Taft substituent parameters ($E_s(-R)$ and $\sigma^*(-R)$) and the Taft reaction (ρ_X^{MeOH} , δ_X^{MeOH} and Ψ_X^{MeOH}) parameters were supposed to be temperature-independent, because the temperature range was relatively small.

2.4.2. KAT equation

There is a distinction between non-specific and specific solute-solvent interactions in the KAT approach. The latter interaction, i.e., the solute-solvent specific interactions, comprises solvent Lewis-acidity and solvent Lewis-basicity interactions. The relationship between the rate constant in a solvent k_X^{Solvent} and the solvent properties is expressed in Eq. (2) (Kamlet et al., 2007; Weiß et al., 2021; Nikolić et al., 2010).

$$\ln(k_X^{\text{Solvent}}) = A_{0,X} + s_X \cdot \pi^{*,\text{Solvent}} + a_X \cdot \alpha^{\text{Solvent}} + b_X \cdot \beta^{\text{Solvent}} \quad (2)$$

where, $\pi^{*,\text{Solvent}}$, α^{Solvent} and β^{Solvent} are solvatochromic solvent pa-

rameters, assumed to be temperature-independent. The parameter $\alpha^{Solvent}$ measures the hydrogen-bond donor (HBD) acidity of a solvent. The parameter $\pi^{*,Solvent}$ is a solvent index representing its ability to stabilize a charge via the dielectric effect. The solvatochromic parameter $\beta^{Solvent}$ measures the solvent hydrogen-bond acceptor (HBA) basicity.

The term $A_{0,X}$ is the regression value, representing the rate constant in methanol reaction medium. The regression coefficients (a_X , b_X , and s_X) present the relative susceptibilities of the solvent dependence of $\ln(k_{X,-R}^{Solvent})$ to the solvent parameters. Table 3 displays the solvatochromic solvent parameters for each solvent/environmental condition used in this study (Wang et al., 2019; Islam et al., 2020; Brändström, 1999; MacPhee et al., 1978; Dubois et al., 1980; Panaye et al., 1980; Jessop et al., 2012).

From Table 3, one can notice that all these alcohols have similar abilities to donate hydrogen bonds ($\beta^{Solvent}$). However, their abilities to accept hydrogen bonds ($\alpha^{Solvent}$) vary, with methanol and ethanol showing higher values than the longer-chain alcohols. Additionally, polarizability ($\pi^{*,Solvent}$) tends to decrease as the carbon chain length increases.

The reaction rate of 5-HMF by ROH reactant in an alcohol reaction medium can be expressed as

$$\ln(k_{X,-R}^{ROH}) = A_{0,X} + s_X \cdot \pi^{*,ROH} + a_X \cdot \alpha^{ROH} + b_X \cdot \beta^{ROH} \quad (3)$$

The reaction rate of 5-HMF by ROH reactant in methanol reaction medium by using KAT relationships is

$$\ln(k_{X,-R}^{MeOH}) = A_{0,X} + s_X \cdot \pi^{*,MeOH} + a_X \cdot \alpha^{MeOH} + b_X \cdot \beta^{MeOH} \quad (4)$$

In Eqs. (3) and (4), the term A_0 , s_X , a_X and b_X are the same, and by subtracting both relationships, we get

$$\ln(k_{X,-R}^{ROH}) - \ln(k_{X,-R}^{MeOH}) = s_X \cdot (\pi^{*,ROH} - \pi^{*,MeOH}) + a_X \cdot (\alpha^{ROH} - \alpha^{MeOH}) + b_X \cdot (\beta^{ROH} - \beta^{MeOH}) \quad (5)$$

The kinetic terms $\ln(k_{X,-R}^{MeOH})$ can be determined from Taft equation, i. e., Eq. (1):

$$k_{X,-R}^{MeOH} = k_{X,-Me}^{MeOH} \cdot 10^{\rho_X^{*,MeOH} \cdot \sigma^*(-R) + \delta_X^{MeOH} \cdot E_s(-R)} \quad (6)$$

Combination of Eqs. (5) and (6) leads to

$$\ln(k_{X,-R}^{ROH}) = \ln(k_{X,-Me}^{MeOH}(T) \cdot 10^{\rho_X^{*,MeOH} \cdot \sigma^*(-R) + \delta_X^{MeOH} \cdot E_s(-R)}) + s_X \cdot (\pi^{*,ROH} - \pi^{*,MeOH}) + a_X \cdot (\alpha^{ROH} - \alpha^{MeOH}) + b_X \cdot (\beta^{ROH} - \beta^{MeOH}) \quad (7)$$

Table 3

Taft and solvatochromic parameters (Wang et al., 2019; Islam et al., 2020; Brändström, 1999; MacPhee et al., 1978; Dubois et al., 1980; Panaye et al., 1980; Jessop et al., 2012).

Alkyl substituent	$\sigma^*(-R)$	$E_s(-R)$	α	β	π	Alcohol
CH ₃ -	0	0	0.98	0.7	0.6	Methanol
CH ₃ -CH ₂ -	-0.1	-0.07	0.86	0.8	0.54	Ethanol
CH ₃ -CH ₂ -CH ₂ -	-0.115	-0.36	0.84	0.85	0.53	n-Propanol
CH ₃ -(CH ₂) ₂ -CH ₂ -	-0.13	-0.39	0.79	0.84	0.47	n-Butanol
CH ₃ -(CH ₂) ₃ -CH ₂ -	-0.15	-0.4	0.84	0.86	0.4	n-Pentanol
CH ₃ -(CH ₂) ₄ -CH ₂ -	-0.124	-0.44	0.80	0.84	0.4	n-Hexanol

3. Experimental results and discussion

3.1. Phenomenological description

The solvolysis of 5-HMF to alkyl levulinates was performed in (H₂O, MeOH, EtOH, PrOH, BuOH, PeOH, HeOH) reaction medium, keeping an alcohol/GVL system of 70/30 wt% ratio over different temperature conditions, initial concentration and catalyst loading. The normalized concentration profiles of each species (Fig. 2) are displayed, except for formic acid (FA). Due its high volatility and low stability, it was not possible to track the concentration of FA.

Kinetic results from Runs 1, 2, 3, 5, 7, 9, and 17 were compared for this section.

Fig. 2A shows that the consumption rate of 5-HMF with short carbon chain alcohols is the most rapid, notably for methanol and ethanol. Nevertheless, there is no explicit relationship between the number of carbon and the consumption rate; for instance, the 5-HMF generation rate is slightly faster for hexanol than propanol. One must observe that the consumption rate of 5-HMF in water reaction medium is very slow compared to that of other alcohol reaction medium in the same operating conditions. For example, after 420 minutes of reaction, ca. 20 % of the initial 5-HMF is converted into water reaction medium compared to almost 100 % for the other alcohol reaction medium.

From Fig. 2B, one can determine the generation rate for 5-RMF, intermediate produced from 5-HMF etherification, which is a balance between its rate of formation and consumption. From this figure, one can observe that the generation rate evolves in the following order: $r_{MMF}^{MeOH} > r_{EMF}^{EtOH} > r_{PMF}^{PrOH} > r_{BMF}^{BuOH} > r_{PeMF}^{PeOH} > r_{HeMF}^{HeOH}$, showing a relationship between the number of carbon and the kinetics. The etherification of 5-HMF with HeOH, PeOH, BuOH produces a high yield of HeMF, PeMF and BMF compared to MMF, EMF, PMF. This is due to the higher thermal stability of HeMF and PeMF.

Fig. 2C shows the production rate of RL, and these rates evolve in the following order $r_{ML}^{MeOH} > r_{EL}^{EtOH} > r_{PL}^{PrOH} > r_{BL}^{BuOH} > r_{PeL}^{PeOH} > r_{HeL}^{HeOH} > r_{LA}^{H_2O}$. This order agrees with the ones for the generation rate of 5-RMF.

In 5-HMF hydrolysis (Fig. 2A) we observe that the 5-HMF conversion with water is quite slow as well the production of LA (Fig. 2C). This result agrees with the ones obtained by Di Menno Di Bucchianico et al. with butanol (Di Menno Di Bucchianico et al., 2022a, 2022b). They reported that the mix of butanol/water did not result in a great conversion of fructose nor a better production of butyl levulinate (BL). The production of LA from the solvolysis of 5-HMF can be considered negligible under the studied experimental conditions since no water is added or present in the reaction system. Hence, the LA production from 5-HMF was neglected during experiments in alcohol reaction medium in the developed models.

From Fig. 2, one can also observe no explicit relationships between the carbon chain from the alcohol and the solvolysis kinetics. Hence, it is necessary to test the Taft equation corrected by the KAT equation to consider the solvent effect.

4. Kinetic modeling

The reaction mechanism of 5-HMF solvolysis remains elusive and is still under debate, essentially from the ring-opening step of 5-HMF or 5-RMF to LA or RL. The first proposed pathway consists of the 5-HMF etherification to RMF and its further conversion to alkyl levulinates; according to some publications on quantum chemical simulations, this route is considered the thermodynamic and kinetic primary way in the solvolysis of hexoses sugar monomers (glucose, fructose) (Wang et al., 2021). The second one requires the hydrolysis of 5-HMF to produce LA, FA and further esterification to alkyl levulinates. Previous studies from our group show that the production of LA is mainly favored by the presence of water (Di Menno Di Bucchianico et al., 2022b).

For the kinetic modeling of the 5-HMF solvolysis, a combination of

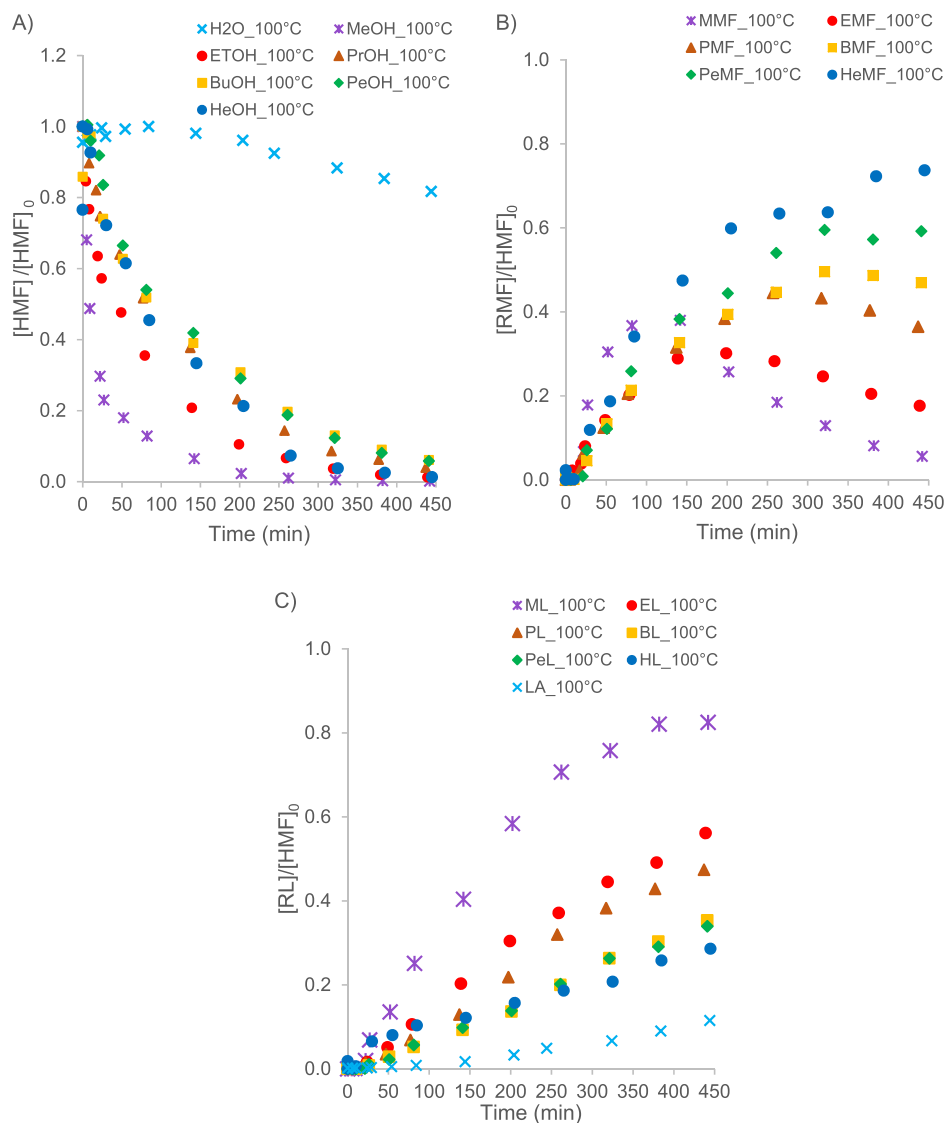


Fig. 2. Reaction medium effect on the solvolysis of 5-HMF at 100°C.

Taft and KAT equations was applied in one model to aid the kinetic prediction in different reaction medium and substituents. Methanol was used as a reference reaction medium and substituent.

From our experimental results, we noticed that the production of LA can be neglected during experiments carried out in alcohol reaction medium. The experimental concentrations of 5-HMF, 5-RMF and RL were used as observables.

Based on some recent publications (Wang et al., 2021; Guo et al., 2020), the first reaction is the protonation of the alcohol by the acid catalyst, and then the hydroxyl group from 5-HMF performs a nucleophile substitution.

In the developed models, we omitted the solvolysis in water reaction medium of 5-HMF into LA and FA, because the reaction steps could differ. Indeed, the literature mentions that the first step is the protonation of the hydroxyl group, leading to dehydration for the 5-HMF solvolysis by water.

Another challenge is the kinetic description of humins production from 5-HMF (Liu et al., 2022). We did not track the humins concentration analytically, but from the mass balance, its presence varied from 0 % to 25 % according to the solvent nature (Table S1 of the Supplementary Data). The reaction steps explaining the humins production are also unclear, but it is linked to the reactivity of the hydroxyl group of

5-HMF, which does not exist in 5-RMF (Sun et al., 2020; Guo et al., 2017; Karnjanakom et al., 2019). Thus, humins production comes solely from the degradation of 5-HMF.

Hence, we developed four global kinetic models. Fig. 3. shows the reaction pathway for Models 1 and 2. Model 1 excludes the presence of humins, and Model 2 includes the production of humins. Model 2 results are displayed in Supplementary Data (Section S3). Model 3 assumed that there are no intermediates (Section S4 of the Supplementary Data). Model 4 proposed an intermediate between 5-RMF and RL (Section S5 of the Supplementary Data).

The developed global Model 1 gave the best statistical results, so we presented its results in the main document. In Fig. 3, the species Int1 is a hypothetical intermediate.

Global kinetic models were carried out using the commercial software Athena Visual Studio (Stewart and Caracotsios, 2008, 2010). The ordinary differential equations (ODEs), i.e., Eqs. (11)–(12), derived from material balances were solved out by DDAPLUS solver using a modified Newton algorithm. Athena Visual Studio uses a Bayesian framework. Literature shows that Bayesian framework is better for a multiresponse system than the non-linear least squares one (Kopyscinski et al., 2012; Stewart et al., 1992). Box and Draper found a way to minimize the determinant criterion used as an objective function (OF), Eq. (8), in

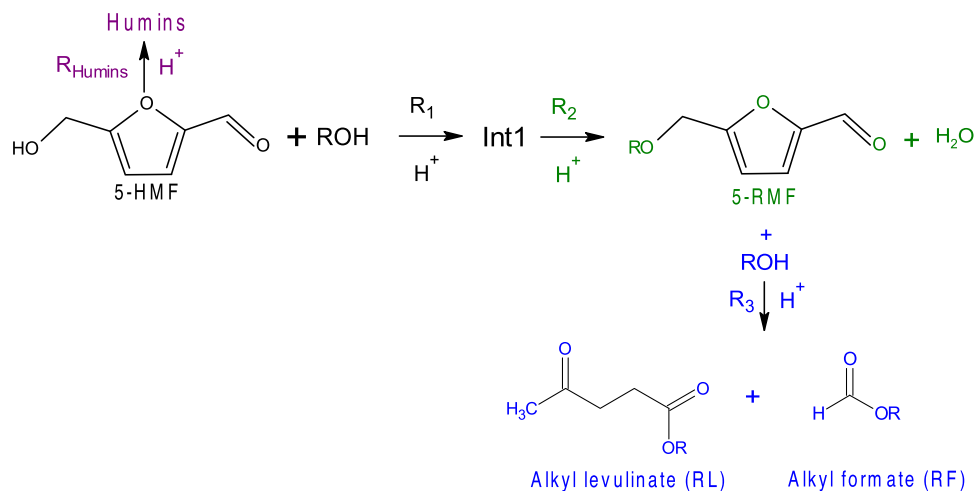


Fig. 3. Reaction steps for the solvolysis of 5-HMF in alcohol reaction medium (Models 1 and 2).

Bayesian framework for multiresponse chemical systems (Box and Draper, 1965; van Boekel, 2020). Athena Visual Studio implemented the GREGPLUS subroutine, which minimizes the OF. GREGPLUS also calculates the credible intervals for each estimated parameter and the normalized parameter covariance.

$$OF = (\gamma + \zeta + 1) \cdot \ln(|\nu|) \quad (8)$$

where $|\nu|$ is the determinant of the covariance matrix of the responses, γ is the number of responses, and ζ is the number of events in response.

Each element of this matrix is as follows:

$$\nu_{ij} = \sum (y_{iu} - \widehat{y}_{iu}) \cdot (y_{ju} - \widehat{y}_{ju}) \quad (9)$$

where y_{iu} is the experimental concentration or temperature and \widehat{y}_{iu} is the estimated value for response i and event u ; and y_{ju} the experimental data and \widehat{y}_{ju} the estimated value for response j and event u .

The minimization of the OF is done via successive quadratic programming. The credible intervals of the estimated parameters were evaluated by the marginal highest posterior density (HPD).

A modified Arrhenius equation was used as suggested by Buzzi-Ferraris (Buzzi-Ferraris, 1999)

$$\ln(k_i(T)) = \ln(k_i(T_{ref})) + \frac{E_{a,i}}{R \cdot T_{ref}} \cdot \left(1 - \frac{T_{ref}}{T}\right) \quad (10)$$

where, $E_{a,i}$ is the activation of reaction i , R is the universal gas constant, T_{ref} is a reference temperature and T is the reaction temperature. The use of Eq. (10) decreases the correlation between the rate constant and activation energy.

4.1. Kinetics for Model 1

Rate expression for steps 1–3 were expressed as

$$R_1^{ROH} = k_1^{ROH} [H^+] [5HMF] [ROH] \quad (11)$$

$$R_2^{ROH} = k_2^{ROH} [H^+] [Int1] \quad (12)$$

$$R_3^{ROH} = k_3^{ROH} [H^+] [RMF] [ROH] \quad (13)$$

$$R_{Humins}^{ROH} = k_{Humins}^{ROH} [H^+] [5HMF] \quad (14)$$

Rate constants k_1^{ROH} , k_2^{ROH} and k_3^{ROH} were expressed via Eq. (7).

The humins production does not incorporate the alcohol ROH or other R- species in its expression, thus, Eq. (5) was used to express the rate constant of humins in different alcohol reaction medium.

$$\ln(k_{Humins}^{ROH}) = \ln(k_{Humins}^{MeOH}) + s_{Humins} \cdot (\pi^{*,ROH} - \pi^{*,MeOH}) + a_{Humins} \cdot (\alpha^{ROH} - \alpha^{MeOH}) + b_{Humins} \cdot (\beta^{ROH} - \beta^{MeOH}) \quad (15)$$

All the reaction steps were considered irreversible. The reaction steps were considered catalyzed by the Amberlite IR-120 H⁺, in which a pseudo-homogeneous approach was used to model the proton catalytic activity (Di Menno Di Bucchianico et al., 2023). The proton concentration was evaluated based in the acid capacity of the Amberlite IR-120 H⁺, i.e., 4.4 meq of protons per dried catalyst mass.

In the non-linear regression stage, the following parameters were estimated:

$$\ln(k_{X,-R}^{MeOH}(T_{ref})); \quad \frac{E_{a,X}^{MeOH}}{R \cdot T_{ref}}; \rho_X^{*,MeOH}; \delta_X^{MeOH}; s_X; a_X; b_X;$$

$$\ln(k_{Humins}^{MeOH}(T_{ref})) \text{ and } \frac{E_{a,Humins}^{MeOH}}{R \cdot T_{ref}}$$

4.2. Material balance for Model 1

Ideal flow conditions were assumed to be. Thus, material balances for each species can be derived as follows:

$$\frac{d[5HMF]}{dt} = -R_1^{ROH} \quad (16)$$

$$\frac{d[RMF]}{dt} = R_1^{ROH} - R_2^{ROH} \quad (17)$$

$$\frac{d[Int1]}{dt} = R_2^{ROH} - R_3^{ROH} \quad (18)$$

$$\frac{d[RL]}{dt} = R_3^{ROH} \quad (19)$$

$$\frac{d[RF]}{dt} = R_3^{ROH} \quad (20)$$

$$\frac{d[ROH]}{dt} = -R_1^{ROH} - R_3^{ROH} \quad (21)$$

4.3. Kinetic modeling results

Fig. 4. shows the fit of Model 1 to experimental concentrations for different reaction medium. In general, Model 1 can fit the experimental concentration correctly. Model 1 can correctly fit the experimental 5-HMF concentration in different reaction medium, except for methanol, that could be due to the fast reaction of 5-HMF consumption in this reaction medium. For the species 5-RMF, the fit is good for species and slightly lower for 5-MMF, which could be linked to faster kinetics

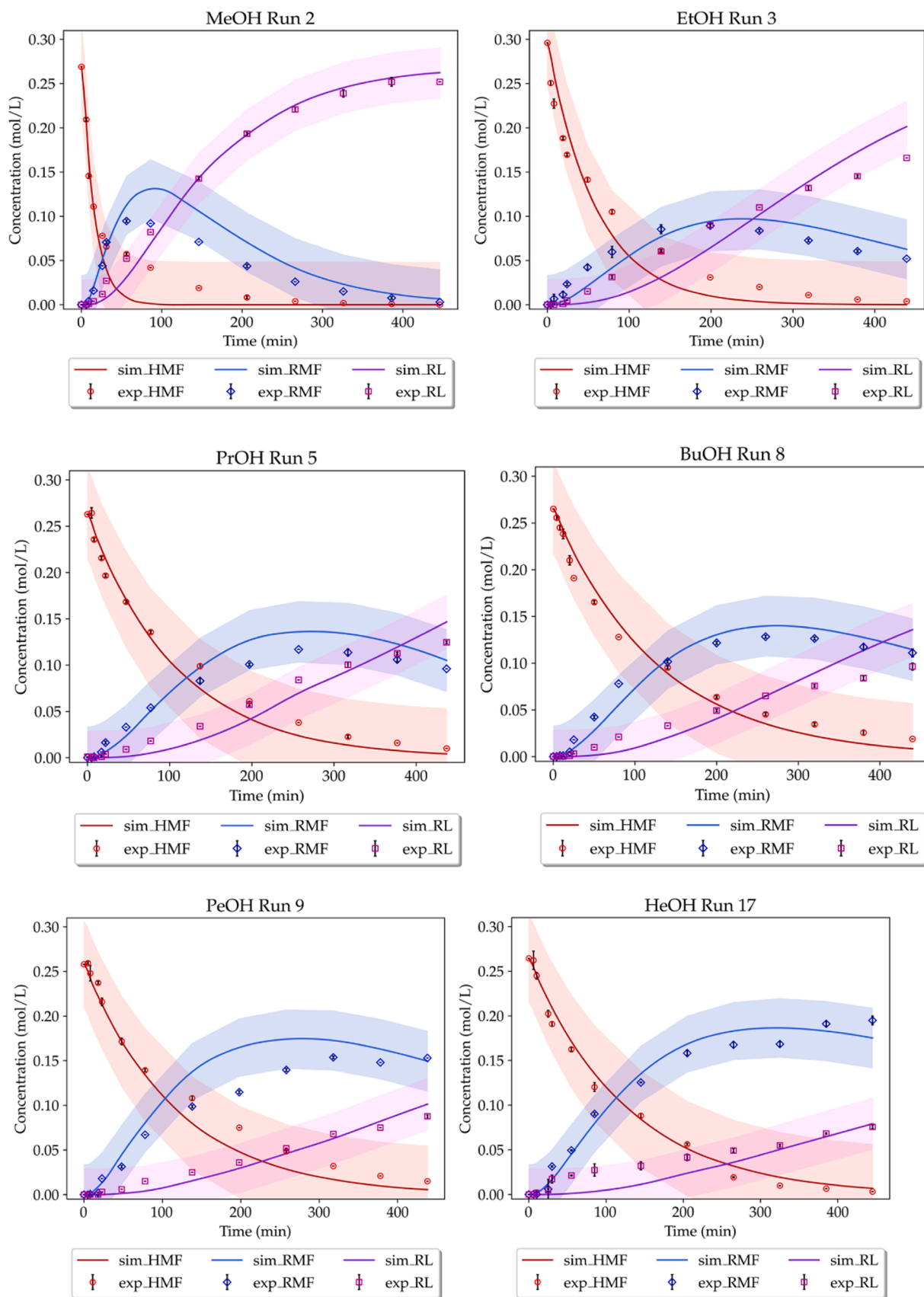


Fig. 4. Fit of Model 1 to experimental concentrations with $\pm 95\%$ prediction intervals.

compared to the other reaction media. Model 1 can correctly fit experimental levulinic concentrations, even if in the case of ethanol, propanol and butanol, there are some slight overestimations at the end, which could be linked to side reactions (e.g., production of humins or ether). Fig. 4 shows that all experimental concentrations are within the 95 % prediction intervals bands (Smith, 2013). It indicates that the observed data are consistent with the model predictions.

Fig. 5 shows the parity plot for each species, showing the excellent agreement of the kinetic model and experimental data. The main difficulty comes from the prediction of the intermediate RMF, which is slightly lower compared to 5-HMF and RL.

Fig. 6 shows the normal probability plots, and one can observe that the relationships between residuals and normal order of statistic median is linear. This linearity proves that the residuals are normally distributed, so Model 1 is appropriately expressed.

Table 4 displays the estimated kinetic constant values and the HPD values, i.e., credible intervals, in percentage. In general, one can notice that credible intervals for KAT parameter (a_x, b_x and s_x) and Taft reaction parameter in methanol reaction medium (ρ_x^{*MeOH} and δ_x^{MeOH}) are wider than the other. These wider credible intervals could be explained by the fact that temperature effect on KAT and Taft substituent and reaction parameters was assumed to be negligible, and the effect of GVL on the solvatochromic parameters was not considered (Table 3). Besides, the solvatochromic parameters α^{ROH} , β^{ROH} and π^{*ROH} of the used alcohols (Table 3) are quite similar, making the estimation of a_x, b_x and s_x more

challenging.

For reactions 1 and 2, the substituent polar effect is more critical than the steric effect, because the Taft reaction parameters ρ_1^{*MeOH} and ρ_2^{*MeOH} are higher than δ_1^{MeOH} and δ_2^{MeOH} . Nevertheless, in reaction 1, the substituent polar effect decreases reaction kinetics 1; in reaction 2, the polar substituent effect increases the kinetics of reaction 2. In reaction 1, if σ_{R-}^* increases, then the substituent R- could stabilize the species $R-(OH_2)^+$ decreasing the kinetics of etherification.

For reaction 3, the steric effect governs the series of transformation of the intermediate to RL and RF in methanol reaction medium. The value of δ_3^{MeOH} is negative, meaning that the higher the substituent group, the faster is reaction 3.

The reader should keep in mind that the estimated Taft reaction parameters, ρ_x^{*MeOH} and δ_x^{MeOH} , for reactions 1–3 were done in methanol reaction medium.

We need to analyze the KAT parameters. In general, the kinetics of reactions 1, 2 and 3 are mainly affected by the hydrogen-bond donor aspect of the solvent, i.e., a_x . For reactions 1 and 3, the value a_x is negative meaning that solvent with high ability to donate protons decreases the rate constants k_1^{ROH} and k_3^{ROH} . This is undoubtedly due to the fact that the protons stabilize the intermediates and thus decrease the kinetics, as observed in the article of Mellmer et al (Mellmer et al., 2014).

In Supplementary Data, in section S2, the normalized covariance

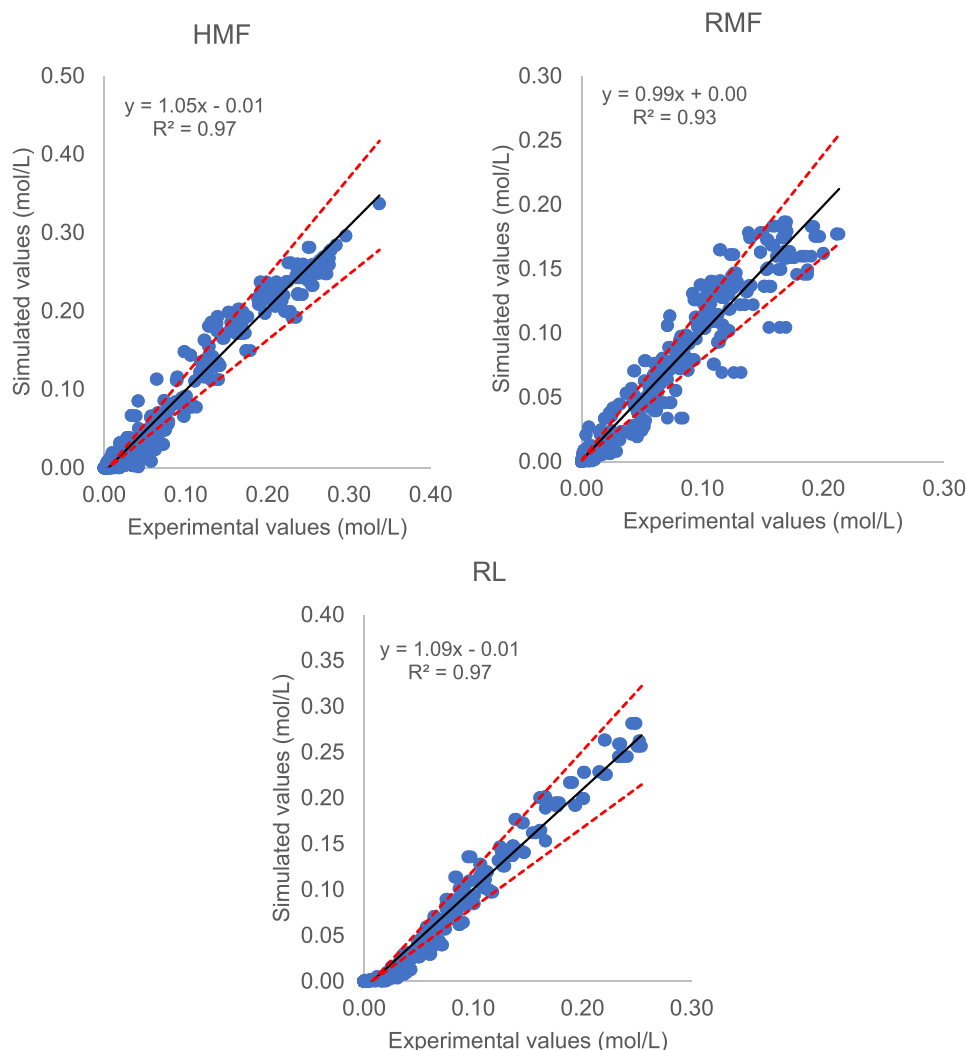


Fig. 5. Parity plots from Model 1 with error lines $\pm 20\%$ (in red).

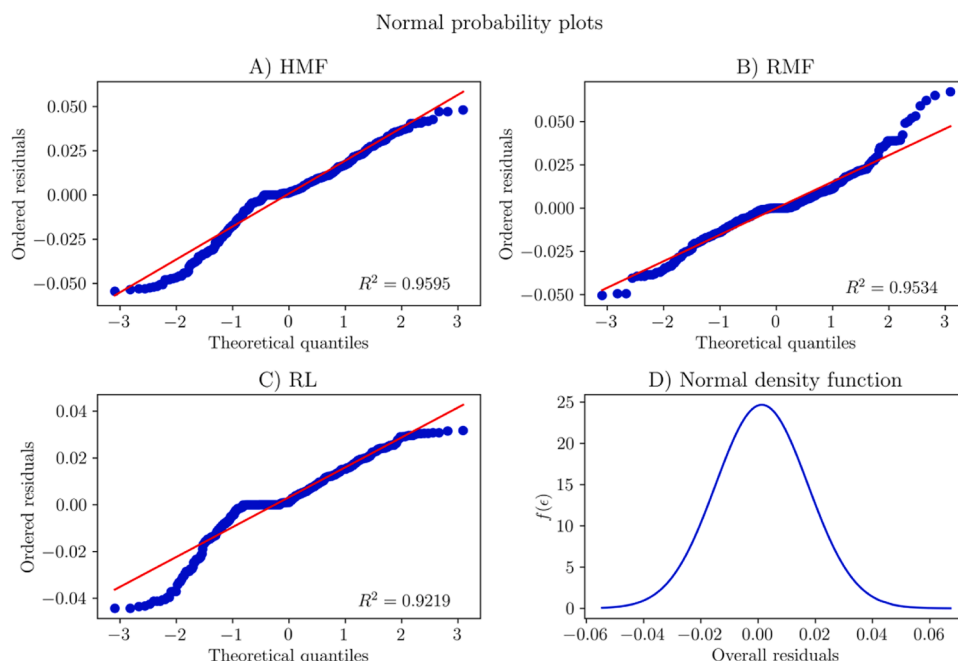


Fig. 6. Normal probability plots for Model 1.

Table 4

Estimated kinetic constants and HPD values and $T_{ref} = 105\text{ }^{\circ}\text{C}$.

Parameters	Estimate	Units	95 % HPD in %
$\ln(k_{1,Me}^{MeOH}(T_{ref}))$	-6.036	$\frac{\text{mol}^{-1}\text{L}^2}{\text{min} \cdot g_{dried\ cat}}$	8.22
$\frac{E_{a,1,Me}^{MeOH}}{RT_{ref}}$	2.421	$\frac{\text{J} \cdot \text{mol}^{-1}}{\text{J} \cdot \text{mol}^{-1} \cdot \text{K}^{-1} \cdot \text{K}}$	40.28
$\ln(k_{2,Me}^{MeOH}(T_{ref}))$	-7.802	$\frac{\text{min}^{-1}\text{L}}{g_{dried\ cat}}$	19.18
$\frac{E_{a,2,Me}^{MeOH}}{RT_{ref}}$	10.197	$\frac{\text{J} \cdot \text{mol}^{-1}}{\text{J} \cdot \text{mol}^{-1} \cdot \text{K}^{-1} \cdot \text{K}}$	16.34
$\ln(k_{3,Me}^{MeOH}(T_{ref}))$	-4.032	$\frac{\text{mol}^{-1}\text{L}^2}{\text{min} \cdot g_{dried\ cat}}$	12.32
$\frac{E_{a,3,Me}^{MeOH}}{RT_{ref}}$	12.853	$\frac{\text{J} \cdot \text{mol}^{-1}}{\text{J} \cdot \text{mol}^{-1} \cdot \text{K}^{-1} \cdot \text{K}}$	8.11
$\rho_1^{*,MeOH}$	3.399	-	84.06
δ_1^{MeOH}	0.393	-	82.32
$\rho_2^{*,MeOH}$	-2.612	-	>100
δ_2^{MeOH}	-2.010	-	41.36
$\rho_3^{*,MeOH}$	-0.174	-	>100
δ_3^{MeOH}	0.963	-	32.56
s_1	2.050	-	62.13
s_2	10.672	-	41.76
s_3	-1.660	-	73.98
a_1	-4.690	-	30.11
a_2	-4.789	-	91.80
a_3	2.121	-	68.36
b_1	-0.806	-	>100
b_2	-9.339	-	>100
b_3	2.865	-	>100

matrix was displayed. One can observe that in the majority the correlation could be assumed negligible, because absolute values were lower than 0.95 in absolute value (Toch et al., 2015). The correlation was found to be strong between some KAT and Taft substituent parameters, namely b_1 and $\rho_1^{*,MeOH}$, and b_2 and $\rho_2^{*,MeOH}$.

5. Conclusions

This manuscript deals with the kinetic study of 5-(hydroxymethyl)

furfural (5-HMF) solvolysis by different alcohols into different alkyl levulinates. Experiments were performed using Amberlite IR-120 as a catalyst and the reaction medium made of alcohol (70 wt%) and GVL (30 wt%). We tested water and the following alcohols: methanol, ethanol, propanol, butanol, pentanol, and hexanol. Preliminary experiments showed that the transformation of 5-HMF to levulinic acid (LA) in water reaction medium was the slowest transformation compared to the other alcohol reaction medium. These preliminary experiments show that the production of 5-HMF and LA is negligible in an alcohol reaction medium. Experimentally, it was found that the rates of alkyl production follow the order: $r_{ML}^{Methanol} > r_{EL}^{Ethanol} > r_{PL}^{Propanol} > r_{BL}^{Butanol} > r_{PeL}^{Pentanol} > r_{HeL}^{Hexanol} > r_{LA}^{Water}$.

Global kinetic models were developed by considering solvent effect, via Kamlet-Abboud-Taft (KAT) equation, and substituent effect, via Taft equation. An experimental matrix was used by varying reaction medium, 5-HMF concentration from 0.20 to 0.30 mol/L, an alcohol concentration from 5.39 to 16.58 mol/L, a catalyst amount from 2.50 to 4.00 g and a reaction temperature from 85 to 110 °C. The developed global kinetic models can predict the experimental concentration of 5-HMF, 5-RMF and RL in alcohol reaction medium. The polar and steric effects characterizing the substituent effect and hydrogen-bond acceptor or donator and solvent polarity provides a better understanding of kinetics, and how to predict the kinetics of the solvolysis of 5-HMF in alcohol reaction medium at different reaction temperature from the knowledge of the kinetics of 5-HMF solvolysis in methanol reaction medium.

This work can be considered as the first brick in this field. A perspective of this work is the evaluation of temperature dependence of the Taft substituent parameters and KAT solvatochromic parameters.

The development of such model considering the solvent effect could ease the process optimization from an economic, environmental and risk standpoints.

CRedit authorship contribution statement

Jean-Christophe Buvat: Writing – original draft, Supervision, Software, Conceptualization. **Julien Legros:** Writing – original draft, Investigation, Conceptualization. **Christoph Held:** Writing – original draft, Methodology, Conceptualization. **Daniele Di Menno Di**

Bucchianico: Writing – original draft, Methodology, Investigation, Formal analysis, Data curation. **Christine Devouge-Boyer:** Writing – original draft, Methodology. **Erny Encarnacion Munoz:** Writing – original draft, Validation, Methodology, Formal analysis, Data curation. **Valeria Casson Moreno:** Writing – original draft, Supervision, Formal analysis, Conceptualization. **sebastien leveneuer:** Writing – review & editing, Writing – original draft, Supervision, Resources, Investigation, Conceptualization.

Declaration of Competing Interest

The authors declare that they have no known competing financial interests or personal relationships that could have appeared to influence the work reported in this paper.

Acknowledgments

The authors thank the Ministry of High Education, Science and Technology of Dominican Republic (MESCYT). For the analytical part, the authors thank INSA Rouen Normandy, University of Rouen Normandy, the Centre National de la Recherche Scientifique (CNRS), European Regional Development Fund (ERDF) No HN0001343, Labex SynOrg (ANR-11-LABX-0029), Carnot Institute I2C, the graduate school for research XL-Chem (ANR-18-EURE-0020 XL CHEM) and Region Normandie for their support. GC/FID was financed by ERDF RIN Green Chem 2019NU01FOBC08 No 17P04374.

This research was funded, in whole or in part, by the ANR (French National Research Agency) and the DFG (German Research Foundation) through the project MUST (Microfluidics for Structure-reactivity relationships aided by Thermodynamics & kinetics) [ANR-20-CE92-0002-01 - Project number 446436621].

Appendix A. Supporting information

Supplementary data associated with this article can be found in the online version at [doi:10.1016/j.cherd.2024.03.040](https://doi.org/10.1016/j.cherd.2024.03.040).

References

- Ahmad, F.B., Kalam, M.A., Zhang, Z., Masjuki, H.H., 2022. Sustainable production of furan-based oxygenated fuel additives from pentose-rich biomass residues. *Energy Convers. Manag.* **X**, 14, 100222 <https://doi.org/10.1016/j.ecmx.2022.100222>.
- Ahmed, M.A., Lee, J.H., Raja, A.A., Choi, J.W., 2020. Effects of Gamma-valerolactone Assisted Fractionation of Ball-milled Pine Wood on Lignin Extraction and Its Characterization as Well as Its Corresponding Cellulose Digestion. *Appl. Sci.* **10**, 1599. <https://doi.org/10.3390/AP10051599>.
- Alibakhshi, A., Hartke, B., 2021. Improved prediction of solvation free energies by machine-learning polarizable continuum solvation model. *Nat. Commun.* **12** (1), 7. <https://doi.org/10.1038/s41467-021-23724-6>.
- Ayub, Y., Zhou, J., Shen, W., Ren, J., 2023. Innovative valorization of biomass waste through integration of pyrolysis and gasification: Process design, optimization, and multi-scenario sustainability analysis. *Energy* **282**, 128417. <https://doi.org/10.1016/j.energy.2023.128417>.
- Baco, S., Klinskiak, M., Ismail Bedawi Zakaria, R., Antonia Garcia-Hernandez, E., Mignot, M., Legros, J., Held, C., Casson Moreno, V., Leveneuer, S., 2022. Solvent effect investigation on the acid-catalyzed esterification of levulinic acid by ethanol aided by a Linear Solvation Energy Relationship. *Chem. Eng. Sci.* **260**, 117928 <https://doi.org/10.1016/j.ces.2022.117928>.
- van Boekel, M.A.J.S., 2020. On the pros and cons of Bayesian kinetic modeling in food science. *Trends Food Sci. Technol.* **99**, 181–193. <https://doi.org/10.1016/j.tifs.2020.02.027>.
- Bond, J.Q., Alonso, D.M., Wang, D., West, R.M., Dumesic, J.A., 2010. Integrated catalytic conversion of γ -valerolactone to liquid alkenes for transportation fuels. *Science* **327** (80), 1110–1114. (https://doi.org/10.1126/SCIENCE.1184362/SUPPL_FILE/BOND.SOM.PDF).
- Box, G.E.P., Draper, N.R., 1965. The Bayesian estimation of common parameters from several responses. *Biometrika* **52**, 355–365. <https://doi.org/10.1093/biomet/52.3-4.355>.
- Brändström, A., 1999. Prediction of Taft's σ^* parameter for alkyl groups and alkyl groups containing polar substituents. *J. Chem. Soc. Perkin Trans. 2*, 1855–1857. <https://doi.org/10.1039/a904819g>.
- Brown, D.W., Floyd, A.J., Kinsman, R.G., Roshan-Ali, Y., 1982. Dehydration reactions of fructose in non-aqueous media. *J. Chem. Technol. Biotechnol.* **32**, 920–924. <https://doi.org/10.1002/jctb.5030320730>.
- Buzzi-Ferraris, G., 1999. Planning of experiments and kinetic analysis. *Catal. Today* **52**, 125–132. [https://doi.org/10.1016/S0920-5861\(99\)00070-X](https://doi.org/10.1016/S0920-5861(99)00070-X).
- Capecci, S., Wang, Y., Casson Moreno, V., Held, C., Leveneuer, S., 2021. Solvent effect on the kinetics of the hydrogenation of n-butyl levulinate to γ -valerolactone. *Chem. Eng. Sci.* **231**, 116315 <https://doi.org/10.1016/j.ces.2020.116315>.
- Caron, S., 2011. *Practical Synthetic Organic Chemistry: Reactions, Principles, and Techniques*. John Wiley and Sons. <https://doi.org/10.1002/9781118093559>.
- Chen, J., Geng, W., Wei, G.W., 2021. MLIMC: Machine learning-based implicit-solvent Monte Carlo. *Chin. J. Chem. Phys.* **34**, 683–694. <https://doi.org/10.1063/1674-0068/cjcp2109150>.
- Chen, B., Xu, G., Chang, C., Zheng, Z., Wang, D., Zhang, S., Li, K., Zou, C., 2019. Efficient one-pot production of biofuel 5-ethoxymethylfurfural from corn stover: optimization and kinetics. *Energy Fuels* **33**, 4310–4321. (https://doi.org/10.1021/ACS.ENERGYFUELS.9B00357/ASSET/IMAGES/MEDIUM/EF-2019-003579_0014.GIF).
- Chithra, P.A., Darbha, S., 2020. Catalytic conversion of HMF into ethyl levulinate – a biofuel over hierarchical zeolites. *Catal. Commun.* **140**, 105998 <https://doi.org/10.1016/j.cattcom.2020.105998>.
- Delidovich, I., Leonhard, K., Palkovits, R., 2014. Cellulose and hemicellulose valorisation: an integrated challenge of catalysis and reaction engineering. *Energy Environ. Sci.* **7**, 2803–2830. <https://doi.org/10.1039/C4EE01067A>.
- Dubois, J.E., Macphee, J.A., Panaye, A., 1980. Steric effects-III: Composition of the E's parameter. Variation of alkyl steric effects with substitution. Role of conformation in determining sterically active and inactive sites. *Tetrahedron* **36**, 919–928. [https://doi.org/10.1016/0040-4020\(80\)80043-3](https://doi.org/10.1016/0040-4020(80)80043-3).
- Flannelly, T., Dooley, S., Leahy, J.J., 2015. Reaction Pathway Analysis of Ethyl Levulinate and 5-Ethoxymethylfurfural from d-Fructose Acid Hydrolysis in Ethanol. *Energy Fuels* **29**, 7554–7565. (https://doi.org/10.1021/ACS.ENERGYFUELS.5B01481/ASSET/IMAGES/EF-2015-01481W_M008.GIF).
- Gerlach, T., Müller, S., de Castilla, A.G., Smirnova, I., 2022. An open source COSMO-RS implementation and parameterization supporting the efficient implementation of multiple segment descriptors. *Fluid Phase Equilib.* **560**, 113472 <https://doi.org/10.1016/j.fluid.2022.113472>.
- Gogoi, D., Kumar, M., Lakshmi, Y.G., 2023. A comprehensive review on “pyrolysis” for energy recovery. *Bioenergy Res* **16**, 1417–1437. <https://doi.org/10.1007/s12155-023-10568-9>.
- Guo, H., Duereh, A., Su, Y., Hensen, E.J.M., Qi, X., Smith, R.L., 2020. Mechanistic role of protonated polar additives in ethanol for selective transformation of biomass-related compounds. *Appl. Catal. B Environ.* **264**, 118509 <https://doi.org/10.1016/j.apcatb.2019.118509>.
- Guo, H., Qi, X., Hiraga, Y., Aida, T.M., Smith, R.L., 2017. Efficient conversion of fructose into 5-ethoxymethylfurfural with hydrogen sulfate ionic liquids as co-solvent and catalyst. *Chem. Eng. J.* **314**, 508–514. <https://doi.org/10.1016/j.cej.2016.12.008>.
- Islam, T., Islam Sarker, M.Z., Uddin, A.H., Yunus, K.B., Prasad, R., Mia, M.A.R., Ferdosh, S., 2020. Kamlet taft parameters: a tool to alternate the usage of hazardous solvent in pharmaceutical and chemical manufacturing/synthesis - a gateway towards green technology. *Anal. Chem. Lett.* **10**, 550–561. <https://doi.org/10.1080/22297928.2020.1860124>.
- Jessop, P.G., Jessop, D.A., Fu, D., Phan, L., 2012. Solvatochromic parameters for solvents of interest in green chemistry. *Green. Chem.* **14**, 1245–1259. <https://doi.org/10.1039/c2gc16670d>.
- Jung, D., Körner, P., Kruse, A., 2021. Kinetic study on the impact of acidity and acid concentration on the formation of 5-hydroxymethylfurfural (HMF), humins, and levulinic acid in the hydrothermal conversion of fructose, *Biomass Convers. Biorefinery* **11**, 1155–1170. <https://doi.org/10.1007/S13399-019-00507-0/FIGURES/14>.
- Kamlet, M.J., Abboud, J.L.M., Taft, R.W., 2007. An examination of linear solvation energy relationships. *Prog. Phys. Org. Chem.* John Wiley & Sons, Ltd, pp. 485–630. <https://doi.org/10.1002/9780470171929.ch6>.
- Karnjanakom, S., Bayu, A., Maneechakr, P., Samart, C., Kongparakul, S., Guan, G., 2021. Rapid transformation of furfural to biofuel additive ethyl levulinate with in situ suppression of humins promoted by an acidic-oxygen environment. *ACS Sustain. Chem. Eng.* **9**, 14170–14179. (https://doi.org/10.1021/ACSUSCHEM.1C04606/ASSET/IMAGES/LARGE/SC1C04606_0011.JPEG).
- Karnjanakom, S., Maneechakr, P., Samart, C., Guan, G., 2019. A facile way for sugar transformation catalyzed by carbon-based Lewis-Bronsted solid acid. *Mol. Catal.* **479**, 110632 <https://doi.org/10.1016/j.mcat.2019.110632>.
- Kopyscinski, J., Choi, J., Hill, J.M., 2012. Comprehensive kinetic study for pyridine hydrogenation on (Ni)WP/SiO₂ catalysts. *Appl. Catal. A Gen.* **445–446**, 50–60. <https://doi.org/10.1016/j.apcata.2012.08.027>.
- Kulkarni, P.U., Shah, H., Vyas, V.K., 2021. Hybrid quantum mechanics/molecular mechanics (QM/MM) simulation: a tool for structure-based drug design and discovery. *Mini-Rev. Med. Chem.* **22**, 1096–1107. <https://doi.org/10.2174/1389557521666211007115250>.
- Leveneuer, S., 2017. Thermal safety assessment through the concept of structure-reactivity: application to vegetable oil valorization. *Org. Process Res. Dev.* **21**, 543–550. <https://doi.org/10.1021/acs.oprd.6b00405>.
- Lilja, J., Murzin, D.Y., Salmi, T., Aumo, J., Maäki-Arvela, P., Sundell, M., 2002. Esterification of different acids over heterogeneous and homogeneous catalysts and correlation with the taft equation. *J. Mol. Catal. A Chem.* **182**, 555–563. [https://doi.org/10.1016/S1381-1169\(01\)00495-2](https://doi.org/10.1016/S1381-1169(01)00495-2).
- Liu, Y., Deak, N., Wang, Z., Yu, H., Hamelers, L., Jurak, E., Deuss, P.J., Barta, K., 2021. Tunable and functional deep eutectic solvents for lignocellulose valorization. *Nat. Commun.* **12**, 1–15. <https://doi.org/10.1038/s41467-021-25117-1>.
- Liu, S., Zhu, Y., Liao, Y., Wang, H., Liu, Q., Ma, L., Wang, C., 2022. Advances in understanding the humins: formation, prevention and application. *Appl. Energy Combust. Sci.* **10**, 100062 <https://doi.org/10.1016/J.JAECS.2022.100062>.

- Lu, Q., Chen, Y., Song, W., Tao, C., Zhang, J., Sun, Y., Peng, L., Liu, H., 2023. Mechanistic role of γ -valerolactone co-solvent to promote ethyl levulinate production from cellulose transformation in ethanol. *Fuel* 346, 128371. <https://doi.org/10.1016/J.FUEL.2023.128371>.
- MacPhee, J.A., Panaye, A., Dubois, J.E., 1978. Steric effects—I: A critical examination of the taft steric parameter—Es. Definition of a revised, broader and homogeneous scale. Extension to highly congested alkyl groups. *Tetrahedron* 34, 3553–3562. [https://doi.org/10.1016/0040-4020\(78\)88431-2](https://doi.org/10.1016/0040-4020(78)88431-2).
- Mellmer, M.A., Sener, C., Gallo, J.M.R., Luterbacher, J.S., Alonso, D.M., Dumesic, J.A., 2014. Solvent effects in acid-catalyzed biomass conversion reactions. *Angew. Chem. - Int. Ed.* 53, 11872–11875. <https://doi.org/10.1002/anie.201408359>.
- Meng, X., Wang, Y., Conte, A.J., Zhang, S., Ryu, J., Wie, J.J., Pu, Y., Davison, B.H., Yoo, C.G., Ragauskas, A.J., 2023. Applications of biomass-derived solvents in biomass pretreatment – strategies, challenges, and prospects. *Bioresour. Technol.* 368, 128280. <https://doi.org/10.1016/j.biortech.2022.128280>.
- Di Menno Di Bucchianico, D., Buvat, J.C., Mignot, M., Casson Moreno, V., Leveueur, S., 2022b. Role of solvent the production of butyl levulinate from fructose. *Fuel* 318, 123703. <https://doi.org/10.1016/j.fuel.2022.123703>.
- Di Menno Di Bucchianico, D., Cipolla, A., Buvat, J.C., Mignot, M., Casson Moreno, V., Leveueur, S., 2022a. Kinetic study and model assessment for n-butyl levulinate production from alcoholysis of 5-(hydroxymethyl)furfural over amberlite IR-120. *Ind. Eng. Chem. Res.* 61, 10818–10836. https://doi.org/10.1021/ACS.IECR.2C01640/ASSET/IMAGES/LARGE/IE2C01640_0004.JPG.
- Di Menno Di Bucchianico, D., Mignot, M., Buvat, J.C., Casson Moreno, V., Leveueur, S., 2023. Production of butyl levulinate from the solvolysis of high-gravity fructose over heterogeneous catalyst: In-depth kinetic modeling. *Chem. Eng. J.* 465, 142914. <https://doi.org/10.1016/J.CEJ.2023.142914>.
- Di Menno Di Bucchianico, D., Wang, Y., Buvat, J.C., Pan, Y., Casson Moreno, V., Leveueur, S., 2022a. Production of levulinic acid and alkyl levulinates: a process insight. *Green Chem.* 24, 614–646. <https://doi.org/10.1039/d1gc02457d>.
- Nikolić, J.B., Ušćumlić, G.S., Jurančić, I.O., 2010. A linear solvation energy relationship study for the reactivity of 2-(4-substituted phenyl)-cyclohex-1-enecarboxylic, 2-(4-substituted phenyl)-benzoic, and 2-(4-substituted phenyl)-acrylic acids with diazodiphenylmethane in various solvents. *Int. J. Chem. Kinet.* 42, 430–439. <https://doi.org/10.1002/KIN.20497>.
- Ning, P., Yang, G., Hu, L., Sun, J., Shi, L., Zhou, Y., Wang, Z., Yang, J., 2021. Recent advances in the valorization of plant biomass. *Biotechnol. Biofuels* 14, 1–22. <https://doi.org/10.1186/s13068-021-01949-3>.
- Panaye, A., MacPhee, J.A., Dubois, J.E., 1980. Steric effects-II. Relationship between topology and the steric parameter. E's-topology as a tool for the correlation and prediction of steric effects. *Tetrahedron* 36, 759–768. [https://doi.org/10.1016/S0040-4020\(01\)93691-9](https://doi.org/10.1016/S0040-4020(01)93691-9).
- Raj, T., Chandrasekhar, K., Banu, R., Yoon, J.J., Kumar, G., Kim, S.H., 2021. Synthesis of γ -valerolactone (GVL) and their applications for lignocellulosic deconstruction for sustainable green biorefineries. *Fuel* 303, 121333. <https://doi.org/10.1016/J.FUEL.2021.121333>.
- Ramli, N.A.S., Amin, N.A.S., 2016. Kinetic study of glucose conversion to levulinic acid over Fe/HY zeolite catalyst. *Chem. Eng. J.* 283, 150–159. <https://doi.org/10.1016/J.CEJ.2015.07.044>.
- Saidi, C.N., Mielczarek, D.C., Paricaud, P., 2020. Predictions of solvation Gibbs free energies with COSMO-SAC approaches. *Fluid Phase Equilib.* 517, 112614. <https://doi.org/10.1016/j.fluid.2020.112614>.
- Sajid, M., Farooq, U., Bary, G., Azim, M.M., Zhao, X., 2021. Sustainable production of levulinic acid and its derivatives for fuel additives and chemicals: progress, challenges, and prospects. *Green Chem.* 23, 9198–9238. <https://doi.org/10.1039/D1GC02919C>.
- Smith, R.C., 2013. Uncertainty quantification: theory, implementation, and applications. *Uncertain. Quantif. Theory, Implement., Appl.* <https://doi.org/10.1137/1.9781611973228>.
- Soh, L., Eckelman, M.J., 2016. Green solvents in biomass processing. *ACS Sustain. Chem. Eng.* 4, 5821–5837. <https://doi.org/10.1021/acsschemeng.6b01635>.
- Stewart, W.E., Caracotsios, M., 2008. Computer-aided modeling of reactive systems. First, N. Jersey. <https://doi.org/10.1002/9780470282038>.
- W.E. Stewart, M. Caracotsios, Athena Visual Studio, (2010). (www.athenavizual.com) (accessed June 10, 2020).
- Stewart, W.E., Caracotsios, M., Sørensen, J.P., 1992. Parameter estimation from multiresponse data. *AIChE J.* 38, 641–650. <https://doi.org/10.1002/aic.690380502>.
- Sun, Y., Sun, K., Zhang, L., Zhang, S., Liu, Q., Wang, Y., Wei, T., Gao, G., Hu, X., 2020. Impacts of Solvents on the Stability of the Biomass-Derived Sugars and Furans. *Energy Fuels* 34, 3250–3261. <https://doi.org/10.1021/acs.energyfuels.9b03921>.
- Sure, R., el Mahdali, M., Plajer, A., Deglmann, P., 2021. Towards a converged strategy for including microsolvation in reaction mechanism calculations. *J. Comput. Aided Mol. Des.* 35, 473–492. <https://doi.org/10.1007/s10822-020-00366-2>.
- Taft, R.W., 1952a. Linear free energy relationships from rates of esterification and hydrolysis of aliphatic and ortho-substituted benzoate esters. *J. Am. Chem. Soc.* 74, 2729–2732. <https://doi.org/10.1021/ja011131a010>.
- Taft, R.W., 1952b. Polar and Steric Substituent Constants for Aliphatic and o-Benzoate Groups from Rates of Esterification and Hydrolysis of Esters. *J. Am. Chem. Soc.* 74, 3120–3128. <https://doi.org/10.1021/ja011132a049>.
- Taft, R.W., 1953a. Linear Steric Energy Relationships. *J. Am. Chem. Soc.* 75, 4538–4539. <https://doi.org/10.1021/ja01114a044>.
- Taft, R.W., 1953b. The Separation of Relative Free Energies of Activation to Three Basic Contributing Factors and the Relationship of These to Structure. *J. Am. Chem. Soc.* 75, 4534–4537. <https://doi.org/10.1021/ja01114a043>.
- Takkellapati, S., Li, T., Gonzalez, M.A., 2018. An overview of biorefinery-derived platform chemicals from a cellulose and hemicellulose biorefinery. *Clean. Technol. Environ. Policy* 20, 1615–1630. <https://doi.org/10.1007/s10098-018-1568-5>.
- Tanoury, G.J., Iyemperumal, S.K., Lee, E.C., 2023. Toward a Combined Molecular Dynamics and Quantum Mechanical Approach to Understanding Solvent Effects on Chemical Processes in the Pharmaceutical Industry: The Case of a Lewis Acid-Mediated SNAr Reaction. *Org. Process Res. Dev.* 27, 742–754. <https://doi.org/10.1021/acs.oprd.3c00010>.
- Toch, K., Thybaut, J.W., Marin, G.B., 2015. A systematic methodology for kinetic modeling of chemical reactions applied to n-hexane hydroisomerization. *AIChE J.* 61, 880–892. <https://doi.org/10.1002/aic.14680>.
- Verma, S., Dregulo, A.M., Kumar, V., Bhargava, P.C., Khan, N., Singh, A., Sun, X., Sindhu, R., Binod, P., Zhang, Z., Pandey, A., Awasthi, M.K., 2023. Reaction engineering during biomass gasification and conversion to energy. *Energy* 266, 126458. <https://doi.org/10.1016/j.energy.2022.126458>.
- Vojtko, J., Tomčík, P., 2014. A method for esterification reaction rate prediction of aliphatic monocarboxylic acids with primary alcohols in 1,4-dioxane based on two parametric taft equation. *Int. J. Chem. Kinet.* 46, 189–196. <https://doi.org/10.1002/kin.20845>.
- Wang, Z., Chen, Q., 2016. Conversion of 5-hydroxymethylfurfural into 5-ethoxymethylfurfural and ethyl levulinate catalyzed by MOF-based heteropolyacid materials. *Green Chem.* 18, 5884–5889. <https://doi.org/10.1039/c6gc01206j>.
- Wang, S., Chen, Y., Jia, Y., Wang, C., Xu, G., Jiao, Y., He, C., Chang, C., Guo, Q., 2022. DFT and dynamic analysis of glucose alcoholysis conversion to 5-ethoxymethylfurfural and ethyl levulinate. *Fuel* 326, 125075. <https://doi.org/10.1016/j.fuel.2022.125075>.
- Wang, S., Chen, Y., Jia, Y., Xu, G., Chang, C., Guo, Q., Tao, H., Zou, C., Li, K., 2021. Experimental and theoretical studies on glucose conversion in ethanol solution to 5-ethoxymethylfurfural and ethyl levulinate catalyzed by a Brønsted acid. *Phys. Chem. Chem. Phys.* 23, 19729–19739. <https://doi.org/10.1039/D1CP02986J>.
- Wang, Y., Cipolletta, M., Vernières-Hassimi, L., Casson-Moreno, V., Leveueur, S., 2019. Application of the concept of Linear Free Energy Relationships to the hydrogenation of levulinic acid and its corresponding esters. *Chem. Eng. J.* 374, 822–831. <https://doi.org/10.1016/j.cej.2019.05.218>.
- Weiß, N., Schmidt, C.H., Thielemann, G., Heid, E., Schröder, C., Spange, S., 2021. The physical significance of the Kamlet-Taft π^* parameter of ionic liquids. *Phys. Chem. Chem. Phys.* 23, 1616–1626. <https://doi.org/10.1039/D0CP04989A>.
- Wu, Y., Wang, H., Peng, J., Ding, M., 2023. Advances in catalytic valorization of cellulose into value-added chemicals and fuels over heterogeneous catalysts. *Catal. Today* 408, 92–110. <https://doi.org/10.1016/j.cattod.2022.08.012>.
- Xue, Z., Zhao, X., Sun, R.C., Mu, T., 2016. Biomass-derived γ -valerolactone-based solvent systems for highly efficient dissolution of various lignins: Dissolution behavior and mechanism study. *ACS Sustain. Chem. Eng.* 4, 3864–3870. https://doi.org/10.1021/ACSUSCHEMENG.6B00639/ASSET/IMAGES/LARGE/SC-2016-00639X_0003.JPG.
- Xu, L., Coote, M.L., 2019. Methods to improve the calculations of solvation model density solvation free energies and associated aqueous p Ka values: comparison between choosing an optimal theoretical level, solute cavity scaling, and using explicit solvent molecules. *J. Phys. Chem. A* 123, 7430–7438. <https://doi.org/10.1021/acs.jpca.9b04920>.
- Xu, L., Coote, M.L., 2022. Recent Advances in Solvation Modeling Applications: Chemical Properties, Reaction Mechanisms and Catalysis. *Annu. Rep. Comput. Chem. Elsevier*, pp. 53–121. <https://doi.org/10.1016/bs.arcc.2022.09.001>.
- Yan, M., Afentou, N., Fokaides, P.A., 2021. The state of the art overview of the biomass gasification technology. *Curr. Sustain. Energy Rep.* 8, 282–295. <https://doi.org/10.1007/s40518-021-00196-2>.
- Yan, K., Yang, Y., Chai, J., Lu, Y., 2015. Catalytic reactions of gamma-valerolactone: a platform to fuels and value-added chemicals. *Appl. Catal. B Environ.* 179, 292–304. <https://doi.org/10.1016/J.APCATB.2015.04.030>.
- Yiin, C.L., Odita, E. bin, Mun Lock, S.S., Cheah, K.W., Chan, Y.H., Wong, M.K., Chin, B.L.F., Quidant, A.T., Loh, S.K., Yusup, S., 2022. A review on potential of green solvents in hydrothermal liquefaction (HTL) of lignin. *Bioresour. Technol.* 364, 128075. <https://doi.org/10.1016/j.biortech.2022.128075>.
- Yu, Z., Lu, X., Xiong, J., Ji, N., 2019. Transformation of levulinic acid to valeric biofuels: a review on heterogeneous bifunctional catalytic systems. *ChemSusChem* 12, 3915–3930. <https://doi.org/10.1002/SSC.201901522>.
- Zhang, H., Yu, Z., Gu, T., Xiang, L., Shang, M., Shen, C., Su, Y., 2020. Continuous synthesis of 5-hydroxymethylfurfural using deep eutectic solvents and its kinetic study in microreactors. *Chem. Eng. J.* 391, 123580. <https://doi.org/10.1016/j.cej.2019.123580>.
- Zheng, X., Zhi, Z., Gu, X., Li, X., Zhang, R., Lu, X., 2017. Kinetic study of levulinic acid production from corn stalk at mild temperature using FeCl3 as catalyst. *Fuel* 187, 261–267. <https://doi.org/10.1016/J.FUEL.2016.09.019>.
- Zhou, M., Doyle, M.P., Chen, D., 2020a. Combination of levulinic acid and sodium dodecyl sulfate on inactivation of foodborne microorganisms: a review. *Crit. Rev. Food Sci. Nutr.* 60, 2526–2531. <https://doi.org/10.1080/10408398.2019.1650249>.
- Zhou, T., McBride, K., Linke, S., Song, Z., Sundmacher, K., 2020b. Computer-aided solvent selection and design for efficient chemical processes. *Curr. Opin. Chem. Eng.* 27, 35–44. <https://doi.org/10.1016/j.coche.2019.10.007>.
- Žula, M., Jasiukaitytė-Grojzdek, E., Grilc, M., Likozar, B., 2023. Understanding acid-catalysed lignin depolymerisation process by model aromatic compound reaction kinetics. *Chem. Eng. J.* 455, 140912. <https://doi.org/10.1016/J.CEJ.2022.140912>.